Biosensors and Bioelectronics 48 (2013) 258–262

Contents lists available at SciVerse ScienceDirect

Biosensors and Bioelectronics

journal homepage: www.elsevier.com/locate/bios

Core–shell structured Ag@C for direct electrochemistry and hydrogen peroxide biosensor applications

Shuxian Mao [a], Yumei Long [a,b,*], Weifeng Li [a,**], Yifeng Tu [a], Anping Deng [a]

[a] College of Chemistry, Chemical Engineering and Materials Science, Soochow University, Suzhou, Jiangsu 215123, PR China
[b] The Key Lab of Health Chemistry and Molecular Diagnosis of Suzhou, PR China

ARTICLE INFO

Article history:
Received 11 February 2013
Received in revised form
28 March 2013
Accepted 15 April 2013
Available online 30 April 2013

Keywords:
Core–shell structured Ag@C
Horseradish peroxidase
Biosensor
Electrochemistry

ABSTRACT

Ag@C core–shell nano-composites have been prepared by a simple one-step hydrothermal method and are further explored for protein immobilization and bio-sensing. The electrochemical behavior of immobilized horseradish peroxidase (HRP) on Ag@C modified indium–tin–oxide (ITO) electrode and its application as H_2O_2 sensor are investigated. Electrochemical and UV–vis spectroscopic measurements demonstrated that Ag@C nano-composites provide excellent matrixes for the adsorption of HRP and the entrapped HRP retains its bioactivities. It is found that on the HRP–Ag@C/ITO electrode, HRP exhibited a fast electron transfer process and good electrocatalytic reduction toward H_2O_2. Under optimum experimental conditions the biosensor linearly responds to H_2O_2 concentration in the range of 5.0×10^{-7}–1.4×10^{-4} M with a detection limit of 2.0×10^{-7} M ($S/N=3$). The apparent Michaelis–Menten constant (K_M^{app}) of the biosensor is calculated to be 3.75×10^{-5} M, suggesting high enzymatic activity and affinity toward H_2O_2. In addition, the HRP–Ag@C/ITO bio-electrode shows good reproducibility and long-term stability. Thus, the core–shell structured Ag@C is an attractive material for application in the fabrication of biosensors due to its direct electrochemistry and functionalized surface for efficient immobilization of bio-molecules.

1. Introduction

Efficient electron transfer between the redox proteins and electrodes is essential for the understanding of mechanism of biological redox reactions and the development of selective bioelectrocatalyst and biosensor (Zeng et al., 2009; Zhao et al., 2008; Xiao et al., 2003). Unfortunately, most redox proteins exhibit low electron transfer rate on conventional electrode due to their embedded prosthetic groups and instability of the biological matrix at electrode surface (Xu et al., 2007; Li et al., 2001; Riklin et al., 1995). On the other hand, redox proteins immobilized on a biocompatible electrode surface could show enhanced stability and electrochemical activity. Therefore, one of the major challenges is to obtain the desirable materials to enhance the electron mediator-free communication between the redox proteins and electrodes in direct electrochemical filed.

It has been reported that nanomaterials are potential in the immobilization of bio-molecules especially enzymes for the fabrication of electrochemical biosensors because of their high effective surface area, enhancement of mass transport, suitable microenvironment and good conductivity (Pumera et al., 2007; Willner et al., 2007). Metal nanoparticles, for example, were once directly used as electroactive labels to prepare electrochemical sensors (Sun et al., 2009; Authier et al., 2001). However, as-prepared nanomaterials usually have relatively inert surfaces, which make surface modification almost unavoidable before use as supports or templates (Caruso, 2001, 2003; Wang et al., 2002).

Recently, core–shell heteronanostructure has attracted significant attention for the applications in many fields including biomedical, electronics, optical, and catalysis (Chaudhuri and Paria, 2012; Karele et al., 2006). Such hybrid structures can possess multifunctional properties, which can be adjusted by changing either the constituting materials or the core to shell ratio (Oldenberg et al., 1998). Therefore, many attempts have been made to achieve core–shell structures with controlled shell chemistry. Among them, carbon coating is one of the most attractive shell layers for its low preparation cost, chemical activity, and biocompatibility (Liu et al., 2010; Wang et al., 2008; Zhu et al., 2009). In particular, the as-formed colloidal carbon shell inherit large numbers of functional groups from the starting materials and have reactive surfaces, which make possible the loading of other functional molecules for further bioassay application (Sun and Li, 2004, 2005).

* Corresponding author at: College of Chemistry, Chemical Engineering and Materials Science, Soochow University, Suzhou, Jiangsu 215123, PR China. Tel./fax: +86 512 65880089.
** Corresponding author. Tel./fax: +86 512 65880089.
E-mail addresses: yumeilong@suda.edu.cn.(Y. Long) liweifeng@suda.edu.cn.(W. Li)

0956-5663/$ - see front matter © 2013 Elsevier B.V. All rights reserved.
http://dx.doi.org/10.1016/j.bios.2013.04.026

In the present work, Ag@C nanocomposite was synthesized through a hydrothermal process and the resulting nano-composite was employed to immobilize horseradish peroxidase (HRP) for the construction of the H_2O_2 biosensor. The direct electrochemical behaviors of HRP on the Ag@C nano-composite (denoted as HRP–Ag@C/ITO electrode) were investigated, and the electrocatalysis of the biosensor toward H_2O_2 was also studied.

2. Experimental

2.1. Materials and reagents

HRP (EC 1.11.1.7, Type II, 300 U/mg) was obtained from Sangon Biotech Co. Ltd. (Shanghai, China). ITO-coated glass plate (1.1 mm thickness, less than 100 Ω) was obtained from Suzhou NSG Electronics Co. Ltd., China. All other reagents were of analytical grade and purchased from Sinopharm Chemical Reagent Co., Ltd. The phosphate buffer solution (PBS, 0.1 M, pH 7.0) was chosen as the supporting electrolyte and doubly distilled water was used throughout the study.

2.2. Preparation of Ag@C core–shell nano-composites

Ag@C nano-composites were synthesized by hydrothermal method modified from previous report (Sun and Li, 2005). A typical process, 2 mL 0.03 M $AgNO_3$ was added to 0.5 M glucose solution (38 mL) under vigorous stirring. The resulting solution was stirred for another 10 min and then transferred into a Teflon-lined autoclave (50 mL in volume), which was sealed and maintained at 180 °C for 4 h. After reaction, the autoclave was cooled to room temperature. The Ag@C core–shell structured particles were collected by centrifugation and washed with water and ethanol several times. Finally, the as prepared products were dried at 60 °C overnight. For comparison, colloidal carbon sphere (CCS) was prepared following a similar procedure in the absence of $AgNO_3$.

2.3. Preparation of the HRP/Ag@C modified electrode

Prior to use, a sheet of ITO glass (10 mm × 10 mm × 1.1 mm) was ultrasonicated with dilute ammonia, absolute ethanol and distilled water for about 15 min, respectively. Enzyme electrode was fabricated by a simple casting method. Firstly, an Ag@C suspension was obtained by dispersing appropriate amount of Ag@C into 10 mL ethanol with the aid of ultrasonication. Then the fresh solution of HRP (2 mg mL^{-1}, dissolved in pH 7.0 PBS) and Ag@C suspensions were mixed with the volume ratio of 2:1. Finally, 15 μL of the HRP/Ag@C suspension was spread onto the surface of ITO glass and dried in refrigerator at 4 °C to prepare HRP/Ag@C/ITO electrode. In control experiment, the CCS/GC electrode was also prepared with the same procedure above.

2.4. Instruments and measurements

The Ag@C core–shell nanocomposites were characterized by scanning electron microscope (SEM, Hitachi s-4700), TEM (FEI Tecnai G20, an acceleration voltage of 200 kV), and FTIR spectroscopy (Prostar LC240). UV–vis absorbance spectra were recorded on a UV–vis spectrophotometer (TU-1810, Beijing, China).

Electrochemical measurements were performed on a CHI611D electrochemical workstation (Chenhua Instruments Co., Shanghai, China). The measurements were based on a conventional three-electrode system, which includes the HRP/Ag@C/ITO electrode as working electrode, a platinum electrode as auxiliary electrode, and a saturated calomel electrode (SCE) as reference electrode, respectively. All measurements were carried out in PBS at room temperature (25 ± 2 °C). Electrochemical impedance spectroscopy (EIS) was performed on a RST5200 electrochemical workstation (Suzhou Risetest Instrument Co. Ltd., China) in a background solution of 0.1 M KCl containing 1.0×10^{-3} M $[Fe(CN)_6]^{3-/4-}$.

3. Results and discussion

3.1. Characterization of the Ag@C nano-composite

The as-prepared Ag@C nano-composite was characterized by XRD and TEM, as shown in Fig. 1A and B. The XRD pattern in Fig. 1A confirms the existence of the face-centered cubic Ag (JCPDS 87-0597) phase, while the broad peak in the 2θ range of 15–35° is attributed to the amorphous carbon. TEM image shown in Fig. 1B clearly demonstrates the core/shell structure of Ag@C nanocomposite, which has the Ag core with diameters in the range of 50–80 nm and carbon shell with thickness about 100 nm. Fig. S1A and B give typical SEM images of colloidal carbon and Ag@C samples. It can be seen that both the samples have spherical particles with similar particle size from 200 nm to 400 nm.

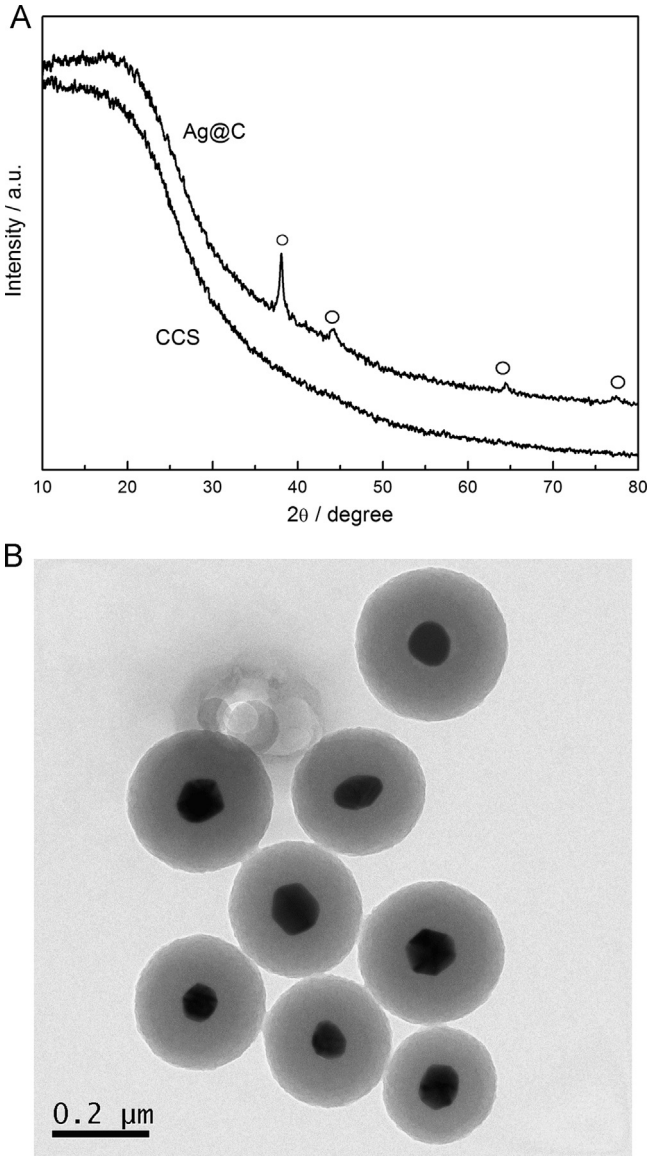

Fig. 1. XRD pattern (A) and TEM image (B) of the Ag@C nanocomposite.

3.2. Spectroscopic analysis

The FT-IR characterization of the Ag@C and CCS was conducted and the spectra were displayed in supporting information as Fig. S2, which can clearly identify the functional groups present after hydrothermal treatment. The signature peaks at about 1710 and 1620 cm^{-1} correspond to C═O and C═C vibrations, respectively. The absorption band ranging from 1000 cm^{-1} to 1300 cm^{-1} is ascribed to the C–OH stretching and OH bending vibrations, which suggests the existence of large numbers of residual hydroxyl groups. Partially dehydrated residues in which reductive OH and CHO are covalently bonded to the carbon frameworks improve the hydrophilicity and stability of the nanospheres in aqueous systems, and greatly widen their potential applications in biochemistry, diagnostics, and drug delivery (Xu et al., 2007). Furthermore, these functional groups outside can enhance the immobility of the Ag@C composites on the ITO glass and improve the absorption to the polar molecules.

The Soret band of protein UV–vis spectrometry is sensitive to the variation of the micro-environment around the heme group and can provide information about the conformational integrity of the proteins. As can be seen from Fig. 2, the Soret absorption of the native HRP and the HRP/Ag@C hybrid is located at nearly the same wavelength (about 403 nm), suggesting that Ag@C nanocomposites have good biocompatibility and do not induce significant denaturation of the HRP in the PBS.

3.3. Electrochemical properties of modified electrode

Fig. 3 shows the typical cyclic valtammagrams (CVs) of different modified electrodes in 0.1 M PBS (H 7.0) at 0.1 V/s. HRP/ITO electrode exhibits slight redox peaks, which could be caused by the deep embedding of the redox-active center of HRP and therefore lead to difficult accessibility for electrons to the electrode surface. On the other hand, The HRP/Ag@C modified electrode shows a pair of well-defined redox peaks. For comparison, CV measurement for HRP/CCS/ITO electrode has also been carried out (curve b in Fig. 3). The electrode also displays a couple of stable redox peaks and the peak current is smaller than that of HRP/Ag@C/ITO one. It may result from the unique core–shell structure of Ag@C, which can provide a desirable microenvironment for HRP to exchange electron with the electrode and enhance the electron transportation.

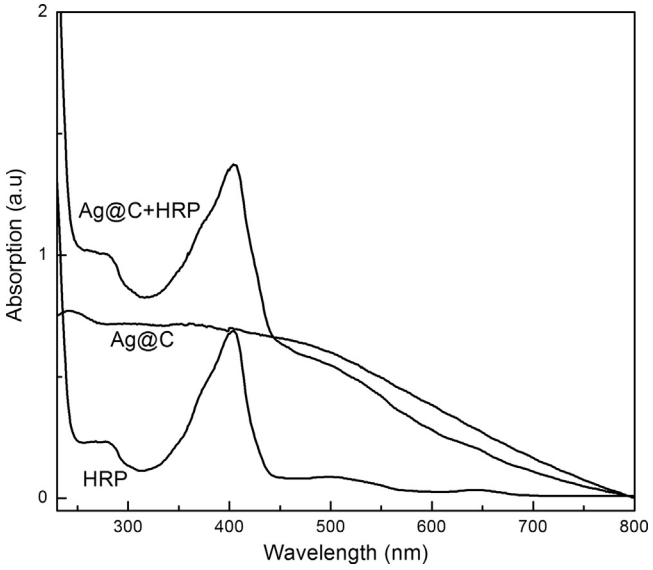

Fig. 2. UV–vis spectra of HRP, HRP/CCS and HRP/Ag@C.

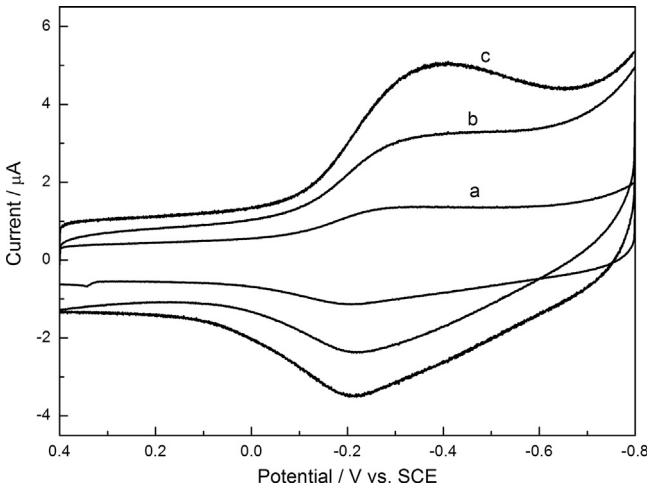

Fig. 3. Cyclic voltammograms of the HRP/ITO (a), HRP/CCS/ITO (b) and HRP/Ag@C/ITO (c) electrodes in 0.1 M pH 7.0 PBS with a scan rate of 0.1 V/s.

The EIS is an effective tool for characterizing the interface properties of surface-modified electrodes. The semicircle diameter in the EIS equals the electron-transfer resistance, R_{et}, which reveals the electron transfer kinetics of the redox electrochemical probe at the electrode interface. Fig. S3 shows the EIS of bare and modified ITO electrodes. The semicircle of the Ag@C-modified ITO electrode (curve b) increases compared with the bare ITO electrode (curve a), which indicates the formation of Ag@C film on the electrode surface and the hindrance effect on the redox couples due to the insulating carbon shell. The adsorption of HRP on Ag@C (curve c) makes the semicircle increase again, suggesting that HRP has been successfully immobilized.

Fig. S4 shows CVs of the HRP/Ag@C/ITO electrode in 0.1 M pH 7.0 PBS at various scan rates. It can be seen that the cathodic and anodic peak currents both increase with increasing scan rates. Moreover, both the cathodic and anodic peak currents are proportional to the square roots of the scan rates, as shown in Fig. S4 inset. It suggests that a diffusion-controlled electrochemical process is involved.

Fig. S5 illustrates the CVs of the HRP/Ag@C/ITO electrode in PBS with different pH values. The optimal sensitivity of the HRP/Ag@C/ITO electrode is achieved at pH 7.0, which is consistent with previous results of HRP-related biosensors (Zhang and Gorski, 2005; Zhao et al., 2008). The slope of the formal potential ($E^{0'}$) versus pH is estimated to be −56 mV/pH (inset of Fig. S5). This value is close to the theoretical value for the transfer of one proton and one electron in a reversible reduction (Wu et al., 2008).

3.4. Electrocatalytic response of the HRP/Ag@C/ITO toward H_2O_2

The electrocatalytic properties of the HRP/Ag@C/ITO electrode were studied by using hydrogen peroxide as a probe. As shown in Fig. 4, the HRP/Ag@C/ITO exhibits a couple of CV peaks in the absence of H_2O_2 (curve a). Upon addition of H_2O_2, the cathodic peak current of immobilized HRP increased and the anodic peak current decreased. The increment of cathodic peak current for higher H_2O_2 concentration (curves b–d) indicated the evident electrocatalytic effect of HRP to the reduction of H_2O_2. The results suggest that the entrapped HRP retains its bioactivity and presents a good electrocatalytic activity toward H_2O_2.

The biosensor performance of the HRP/Ag@C/ITO electrode is also investigated by the amperometric current–time method. Fig. 5 illustrates the *I–t* response on successive addition H_2O_2 to the stirred PBS. The optimal potential and pH value for the amperometric detection are chosen as −0.3 V and 7.0, respectively.

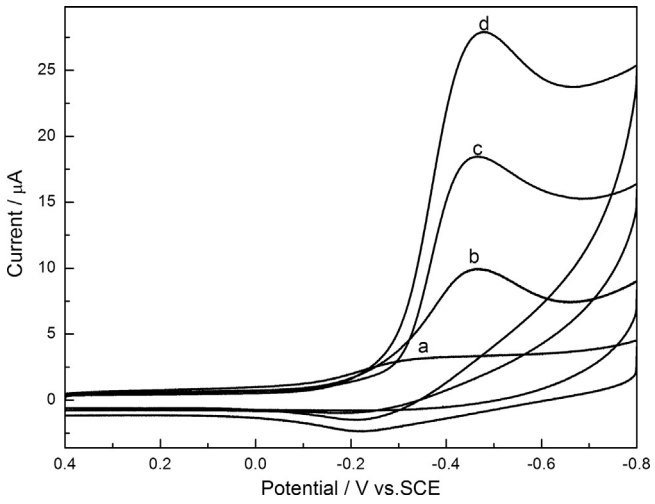

Fig. 4. Cyclic voltammograms of the HRP/Ag@C/ITO in 0.1 M pH 7.0 PBS containing 0 (a), 50 μM (b), 100 μM (c) and 150 μM (d) H_2O_2 with a scan rate of 0.1 V/s.

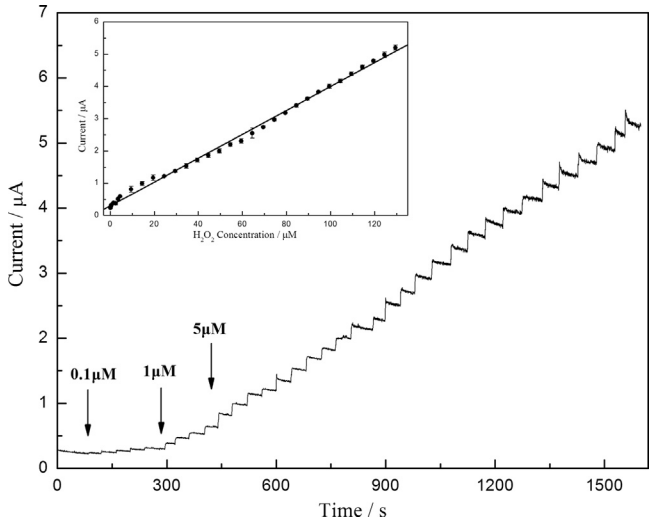

Fig. 5. Current–time response of the HRP/Ag@C/ITO electrode at −0.3 V to successive addition of H_2O_2 in a stirred 0.1 M pH 7.0 PBS. Inset plot: Relationship between the catalytic current and the concentration of H_2O_2. The error bars represent standard deviations based on three independent measurements and the average relative standard deviation is 3.6%.

The current response increases linearly with the increase of H_2O_2 concentration and 95% of the steady-state current is obtained within 3 s. The inset of Fig. 5 shows the linear calibration curve for the detection H_2O_2 using HRP/Ag@C/ITO electrode. The linear range is from 5×10^{-7} to 1.4×10^{-4} M with a correlation coefficient of 0.9985 and the detection limit is estimated to be 0.2×10^{-7} M at signal-to-noise of 3. Based on Lineweaver–Burk equation (Kamin and Willson, 1980), the apparent Michaelis–Menten constant (K_M^{app}) was calculated to be 37.5 μM. The low K_M^{app} value indicates that the HRP immobilized in the Ag@C materials has higher bioactivity and greater affinity to H_2O_2. The comparison of these analytical performances to those recently reported H_2O_2 biosensors was shown in Table S1. It could be seen that the HRP/Ag@C/ITO biosensor are characterized with extended linear range, lower detection limit and good substrate affinity.

3.5. Stability and reproducibility of HRP/Ag@C/ITO biosensor

The long-term stability of the proposed biosensor was valued by measuring its current response in 0.1 mM H_2O_2 after storage at 4 °C for 1 month. The biosensor retained about 92% of its original response. The relative standard deviation of the biosensor response to 0.1 mM H_2O_2 for ten successive determinations was 3.8%. In addition, five freshly prepared HRP/Ag@C/ITO electrodes were employed to measure 0.1 mM H_2O_2. All five electrodes exhibited similar amperometric responses and a relative standard deviation of 4.9% was obtained. The excellent sensing property of HRP/Ag@C/ITO electrode is ascribed to following facts: Firstly, the biocompability of carbon shell can provide a protective microenvironment for the HRP, allowing it to retain its stability and bioactivity; Secondly, rich functional groups in the carbon shell are favorable to the attachment of HRP and prevent the leaking of enzyme from the electrode during the repeated applications; Finally, the good conductivity of Ag core can facilitate the transfer of electron from HRP to electrode.

4. Conclusions

A novel HRP biosensor was developed by immobilizing HRP at Ag@C core–shell structure composite to form a thin film on an ITO electrode. The prepared mediator-free biosensor possesses excellent properties, such as good stability and reproducibility, quick response time, a low detection limit and a high affinity toward H_2O_2 with a wide linear detection range. The enhanced performance of the biosensor can be attributed to the unique structure of Ag@C core–shell structure, whose biocompatible carbon shell can immobilize HRP via functional groups and retain its bioactivity, and Ag core can facilitate the transfer of electron between HRP and electrode. Considering simple fabrication process, the Ag@C core–shell structure has great potential for the development of other enzyme-based biosensors.

Acknowledgments

This work was supported by the National Natural Science Foundation of China (21005053), the Priority Academic Program Development of Jiangsu Higher Education Institutions and The Project of Scientific and Technologic Infrastructure of Suzhou (SZS201207).

Appendix A. Supporting information

Supplementary data associated with this article can be found in the online version at http://dx.doi.org/10.1016/j.bios.2013.04.026.

References

Authier, L., Grossiord, C., Brossier, P., Limoges, B., 2001. Analytical Chemistry 73, 4450–4456.
Caruso, F., 2003. Topics in Current Chemistry 227, 145–168.
Caruso, F., 2001. Advanced Materials 13, 11–22.
Chaudhuri, R.G., Paria, S., 2012. Chemical Reviews 112, 2373–2433.
Kamin, R.A., Willson, G.S., 1980. Analytical Chemistry 52, 1198–1205.
Karele, S., Gosavi, S.W., Urban, J., Kularni, S.K., 2006. Current Science 91, 1038–1052.
Li, Q.W., Luo, G.A., Feng, J., 2001. Electroanalysis 13, 359–363.
Liu, F.X., Cao, Z.S., Tang, C.J., Chen, L., Wang, Z.L., 2010. ACS Nano 5, 2643–2648.
Oldenberg, S.J., Averitt, R.D., Westcott, S.L., Halas, N.J., 1998. Chemical Physics Letters 288, 243–247.
Pumera, M., Sánchez, S., Ichinose, I., Tang, J., 2007. Sensors and Actuators B: Chemical 123, 1195–1205.
Riklin, A., Katz, E., Williner, I., Stockerand, A., Buckmann, A.F., 1995. Nature 376, 672–675.
Sun, H., Choy, T.S., Zhu, D.R., Yam, W.C., Fung, Y.S., 2009. Biosensors and Bioelectronics 24, 1405–1410.
Sun, X.M., Li, Y.D., 2004. Angewandte Chemie International Edition 116, 597–601.
Sun, X.M., Li, Y.D., 2005. Langmuir 21, 6019–6024.
Wang, D.Y., Rogach, A.L., Caruso, F., 2002. Nano Letters 2, 857–861.

Wang, Y.G., Wang, Y.R., Hosono, E., Wang, K.X., Zhou, H.S., 2008. Angewandte Chemie International Edition 47, 7461–7465.
Willner, I., Baron, R., Willner, B., 2007. Biosensors and Bioelectronics 22, 1841–1852.
Wu, F.H., Xu, J.J., Tian, Y., Hu, Z.C., Wang, L.W., Xian, Y.Z., Jin, L.T., 2008. Biosensors and Bioelectronics 24, 198–203.
Xiao, Y., Patolsky, F., Katz, E., Hainfeld, J.F., Willner, I., 2003. Science 299, 1877–1881.
Xu, J.M., Li, W., Yin, Q.F., Zhong, H., Zhu, Y.L., Jin, L.T., 2007. Journal of Colloid and Interface Science 315, 170–176.
Zeng, X., Li, X., Liu, X., Liu, Y., Luo, S., Kong, B., Yang, S., Wei, W., 2009. Biosensors and Bioelectronics 25, 896–900.
Zhang, M.G., Gorski, W., 2005. Journal of American Chemical Society 127, 2058–2059.
Zhao, X.J., Mai, Z.B., Kang, X.H., Zou, X.Y., 2008. Biosensors and Bioelectronics 23, 1032–1038.
Zhu, J.X., Sun, T., Hng, H.H., Ma, J., Boey, F.Y.C., Lou, X.W., Zhang, H., Xue, C., Chen, H. Y., Yan, Q.Y., 2009. Chemistry of Materials 21, 3848–3852.